Nonlinear dynamics of semiflexible magnetic filaments in an ac magnetic field

M. Belovs
University of Latvia, Zellu-8, Riga, Latvia

A. Cēbers*
Institute of Physics, University of Latvia, Salaspils-1, LV-2169, Latvia
(Received 7 March 2006; published 24 May 2006)

Flexible spontaneously magnetized filaments exist in the living world (magnetotactic bacteria) and arise in magnetic colloids with large magnetodipolar interaction parameter. We demonstrate that these filaments possess variety of novel nonlinear phenomena in an ac magnetic field: orientation of the filament in the direction perpendicular to the field and the development of the oscillating U-like shapes, which presumably can lead to the formation of rings of magnetic filaments. It is found that these phenomena are determined by the development of the localized boundary modes of the filament deformation. We have illustrated by qualitative estimates that the phenomena found may be useful for insight into the complex pattern formation phenomena in ensembles of magnetic particles under the action of an ac magnetic field.

DOI: 10.1103/PhysRevE.73.051503 PACS number(s): 83.80.Gv, 87.16.Ka, 87.15.He

I. INTRODUCTION

Magnetic filaments obtained recently in different laboratories [1,2] have caused interest because of the possibility to create artificial colloidal swimmers [3,4], their application for the mixing in microfluidics [5], and other reasons. Their theoretical description is possible on the basis of the model of magnetic semiflexible filament elaborated recently [6]. On this basis, when thermal fluctuations are taken into account, the dispersion of the magnetic susceptibility of spontaneously magnetized filaments is considered [7]. These results show that spontaneously magnetized filament in an ac magnetic field, if its frequency is high enough, should orientate in the direction perpendicular to the field [7]. Similar behavior was observed recently in the vertical ac magnetic field for chains of microne-size Ni particles floating on the surface of the liquid [8]. An interesting point consists in the fact that the model [7] extended for the restoring capillary force on the floating magnetic chain allows one to deduce the mean magnetic energy of the filament, which shows the characteristic minimum in dependence on the length of the filament. This minimum, the position of which depends on the frequency, may correspond to the length of the chainlike aggregates of the ferromagnetic particles floating on the surface of the liquid. A key point for the application of the model of the magnetic semiflexible filament is that the behavior of the chain of the free magnetic particles in the range of the parameters, where the magnetic interaction between them is attractive, can be described by the model of semiflexible filament [9]. Another important issue addressed, when considering the behavior of the magnetic semiflexible filaments in an ac magnetic field, consists in the possibility of the existence of several regimes of stationary oscillations. Here we show by the calculation of the Floquet coefficients and numerical simulation that two distinct stationary regimes of the oscillation of the filament are possible: one with the perpendicular orientation of the filament and oscillations of its tips in phase and another where the body of the filament is parallel to the direction of the applied field but its tips are oscillating in antiphase.

In Sec. II we define our model. There a linear stability analysis is carried out and the existence of the localized boundary modes is illustrated. In Sec. III numerical results of the simulation of the magnetized filament in an ac field are given. The dependence of the amplitude of the filament body orientation angle on the frequency of the ac magnetic field is found. It is verified numerically that in a some range of the parameters two different stationary regimes of the oscillation of the filament—*S* like and *U* like—exist. In Sec. IV the model is generalized to consider the dynamics of the free magnetic particle chains floating on the surface of the liquid. It is shown that the mean magnetic energy of the filament in dependence on its length has a minimum, the position of which depends on the frequency of the ac field. The streaming velocity induced by the oscillating tips of the magnetic filaments is estimated in Sec. V.

II. MODEL

Let us consider a spontaneously magnetized filament with the magnetization per unit length M. The shape of the filament with a curvature elasticity constant C is described by its tangent angle ϑ with a respect to the x axis along which an ac magnetic field $H\cos\omega t$ is applied (Fig. 1). Normal and

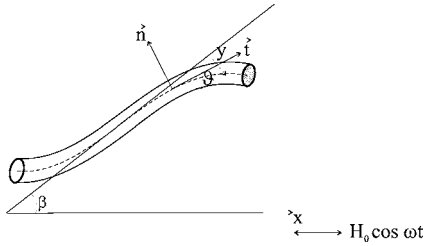

FIG. 1. Picture of a magnetic filament.

*Electronic address: aceb@tesla.sal.lv

tangential components of the stress $\vec{F}$ in the filament are given by [4,6]

$$F_n = C\left(\frac{1}{R}\right)_{,l} + MH\cos\omega t\sin\vartheta, \tag{1}$$

$$F_t = -\left(\frac{C}{2R^2} + \Lambda\right). \tag{2}$$

Here R is the radius of the curvature of the center line of the filament connected with the tangent $\vec{t}$ and the normal $\vec{n}$ according to the Frenet equation $\frac{d\vec{t}}{dl} = -\frac{1}{R}\vec{n}$. Λ characterizes the tension in the filament and is determined from the condition of inextensibility. Partial derivative is denoted by subscript,….

The motion of the filament is considered in the Rouse approximation when the hydrodynamic interaction between its different parts is neglected and the velocity of its material point $\vec{v}$ is

$$\vec{v} = \frac{1}{\zeta}\vec{K},$$

where $\zeta = 4\pi\eta/[\ln(L/a) + c]$ (η is the viscosity of a liquid, c is the constant of order 1), l is the contour length along the filament, $\vec{K} = \frac{d\vec{F}}{dl}$, $2L$ is the length of the filament, and a is the radius of its cross section.

With respect to the Rouse approximation we should remark that due to the mutual influence of the elements of the filament the hydrodynamic drag coefficients along the filament $\zeta_\parallel$ and perpendicular to it $\zeta_\perp$ are different ($\zeta_\perp/\zeta_\parallel \simeq 2$) [10]. Due to this, in general, the velocity of the filament should be expressed as follows:

$$v_n = \frac{1}{\zeta_\perp}K_n, \quad v_t = \frac{1}{\zeta_\parallel}K_t.$$

In the case of small deformations when the tangential motion of the filament is negligible [11] the dynamics is determined by the drag coefficient $\zeta_\perp \equiv \zeta$. The situation is less trivial if the nonlinear effects are important. In some cases—for example, at the motion of the filament in the rotating magnetic field [12]—the account for the anisotropy of hydrodynamic drag coefficients introduces only some quantitative differences in comparison with the isotropic case; for example, the critical frequency for the transition to the nonsynchronous regime in the case $\zeta_\perp/\zeta_\parallel = 2$ is diminished by 50% [13]. Nevertheless, the anisotropy of the hydrodynamic drag does not introduce any qualitative differences in this case. A real situation where the anisotropy of the hydrodynamic drag is essential is the self-propulsion of the flexible filament in an ac magnetic field [3,4,14] when the symmetry between its tips is broken. In this case the self-propelling force is zero if there is no anisotropy of hydrodynamic drag.

The situation with the hydrodynamic drag coefficients is much less clear for the case of the filaments floating on the surface of the liquid. We are aware of the calculations of the drag coefficients of the filaments immersed in the membranes [15] but only for the case when their motion is in the plane of the interface. Nevertheless, for the case considered here of the magnetic particle chains floating on the surface of the liquid and oscillating in the vertical magnetic field [8] the drag coefficient for the motion of the filament perpendicular to the interface is essential. Its calculation could be a formidable problem. At the present moment for the estimates we use its value for the filament in infinite volume of liquid. We hope to improve in this part our estimates in the future. What concerns the anisotropy of the drag coefficients for the ferromagnetic filaments we suppose to take it into account when their self-propulsion in an ac field will be considered. This very intriguing problem is pending for future publications.

To put the equations for the tangent angle and tension Λ in dimensionless form the following scales are introduced: time $\tau = \zeta L^4/C$, tension C/L^2, and length L. As a result the equations in dimensionless form read (the tilde further is omitted)

$$\vartheta_{,t} = -\vartheta_{,llll} - \frac{1}{2}(\vartheta_{,l}^3)_{,l} - (\Lambda\vartheta_{,l})_{,l} + \mathrm{Cm}(\sin\vartheta)_{,ll}\cos\omega t - \vartheta_{,l}\Lambda_{,l} - (\vartheta_{,l})^2\mathrm{Cm}\sin\vartheta\cos\omega t, \tag{3}$$

$$\vartheta_{,l}^2\Lambda - \Lambda_{,ll} = -\vartheta_{,l}\left(\vartheta_{,lll} + \frac{1}{2}(\vartheta_{,l})^3\right) + \mathrm{Cm}\cos\omega t\,\vartheta_{,l}(\sin\vartheta)_{,l} + \mathrm{Cm}\cos\omega t(\vartheta_{,l}\sin\vartheta)_{,l}. \tag{4}$$

Here $\mathrm{Cm} = \frac{MHL^2}{C}$ is the magnetoelastic number and ω characterizes the ratio of the elastic relaxation time and the period of the field. Boundary conditions correspond to the free and unclamped ends of the filament:

$$\vartheta_{,l}\big|_{l=-1,1} = 0,$$

$$\Lambda\big|_{l=-1,1} = 0,$$

$$(\vartheta_{,ll} - \mathrm{Cm}\cos\omega t\sin\vartheta)\big|_{l=-1,1} = 0.$$

A. Linear stability

The nonlinear dynamics of the filament in an ac magnetic field arises due to instability of the filament at the phase of magnetic field when it is directed opposite to the magnetization of the filament. In the case when the magnetic field is constant and opposite to the direction of the magnetization of the filament, its linear stability analysis can be carried out in detail. The linear stability problem reads

$$\vartheta_{,t} = -\vartheta_{,llll} - \mathrm{Cm}\,\vartheta_{,ll}, \tag{5}$$

$$\vartheta_{,l}\big|_{l=-1,1} = 0,\ (\vartheta_{,ll} + \mathrm{Cm}\,\vartheta)\big|_{l=-1,1} = 0. \tag{6}$$

Looking for the solution

$$\vartheta = e^{\lambda t}z(l) = e^{\lambda t}e^{i\beta l},$$

we find

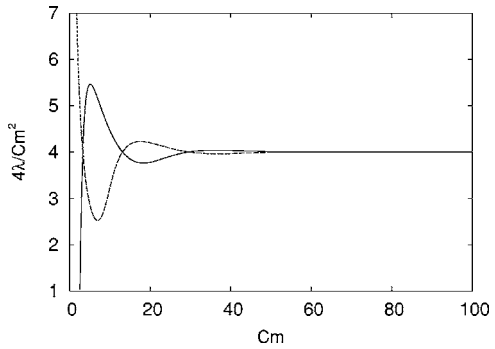

FIG. 2. Increments of the first two modes of the filament deformation.

$$\beta^2 = \frac{\mathrm{Cm} \pm \sqrt{\mathrm{Cm}^2 - 4\lambda}}{2}.$$

Even and odd modes of the filament deformation are analyzed separately.

Introducing

$$\alpha_1 = \sqrt{\frac{1 + \sqrt{1 - 4\lambda/\mathrm{Cm}^2}}{2}}$$

and

$$\alpha_2 = \sqrt{\frac{1 - \sqrt{1 - 4\lambda/\mathrm{Cm}^2}}{2}},$$

the boundary conditions (6) for the even mode,

$$z = A\cos(\sqrt{\mathrm{Cm}}\,\alpha_1 l) + B\cos(\sqrt{\mathrm{Cm}}\,\alpha_2 l),$$

give the dispersion relation

$$\alpha_1(\alpha_2^2 - 1)\sin(\sqrt{\mathrm{Cm}}\,\alpha_1)\cos(\sqrt{\mathrm{Cm}}\,\alpha_2) = \alpha_2(\alpha_1^2 - 1)\cos(\sqrt{\mathrm{Cm}}\,\alpha_1)\sin(\sqrt{\mathrm{Cm}}\,\alpha_2). \quad (7)$$

Equation (7) for the growth increment λ has interesting properties. At $\mathrm{Cm} < 0$ it has no positive solutions, which means that all perturbations are decaying. It has n solutions with $0 < 4\lambda/\mathrm{Cm}^2 < 1$ at $\mathrm{Cm}_{c_{\mathrm{even}}}^{(n+1)} > \mathrm{Cm} > \mathrm{Cm}_{c_{\mathrm{even}}}^{(n)}$ with $\mathrm{Cm}_{c_{\mathrm{even}}}^{(n)} = n^2\pi^2$, and there is one solution with $4\lambda/Cm^2 > 1$ for all Cm.

$\mathrm{Cm}_{c_{\mathrm{even}}}^{(n)}$ defines the critical magnetoelastic number at which the nth deformation mode of the filament is neutral. Mode $n=0$ corresponds to the rotation of the filament as a rigid rod. The increment of the growth of this mode corresponds to the solution of Eq. (7) with $4\lambda/\mathrm{Cm}^2 > 1$. As Cm increases $4\lambda/\mathrm{Cm}^2$ of this mode in a nonmonotonous way approaches 4 as is shown in Fig. 2 by a dashed line.

The odd mode for the tangent angle is considered in the same way. Taking

$$z = A\sin(\sqrt{\mathrm{Cm}}\,\alpha_1 l) + B\sin(\sqrt{\mathrm{Cm}}\,\alpha_2 l),$$

the boundary conditions (6) give the dispersion equation

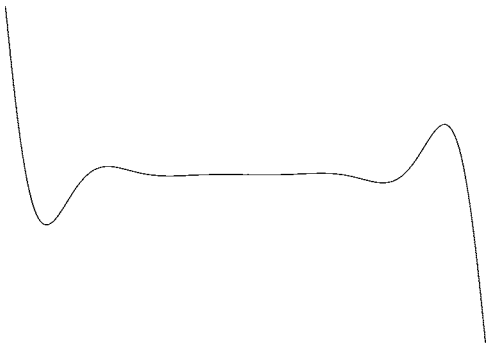

FIG. 3. First even mode of the filament deformation. Cm=200.

$$\alpha_1(\alpha_2^2 - 1)\cos(\sqrt{\mathrm{Cm}}\,\alpha_1)\sin(\sqrt{\mathrm{Cm}}\,\alpha_2) = \alpha_2(\alpha_1^2 - 1)\cos(\sqrt{\mathrm{Cm}}\,\alpha_2)\sin(\sqrt{\mathrm{Cm}}\,\alpha_1). \quad (8)$$

The properties of the solutions of Eq. (8) are the following. If $\mathrm{Cm}_{c_{\mathrm{odd}}}^{(n+1)} > \mathrm{Cm} > \mathrm{Cm}_{c_{\mathrm{odd}}}^{(n)}$ with $\mathrm{Cm}_{c_{\mathrm{odd}}}^{(n)} = (\pi/2)^2(2n+1)^2$ and $\mathrm{Cm} < \mathrm{Cm}_*$, there are n solutions with $0 < 4\lambda/\mathrm{Cm}^2 < 1$. Above the critical value of $\mathrm{Cm}_* = 2.597$ there is one solution with $4\lambda/\mathrm{Cm}^2 > 1$, which corresponds to the eigenvalue of the first odd mode ($n=1$), and $(n-1)$ solutions with $0 < 4\lambda/\mathrm{Cm}^2 < 1$. Cm_* can be found by the solution of the problem (5) and (6) in the case $4\lambda/\mathrm{Cm}^2 = 1$. Then $\alpha_1 = \alpha_2 = \alpha$ and the solution of the problem (5) and (6) reads

$$z = A\sin\alpha l + Bl\cos\alpha l,$$

where $\alpha = \sqrt{\mathrm{Cm}_*/2}$.

The solvability condition of the set of algebraic equations arising due to boundary conditions (6) is the following

$$\alpha(\mathrm{Cm}_* - \alpha^2) = (\alpha^2 + \mathrm{Cm}_*)\sin\alpha\cos\alpha,$$

which gives $\mathrm{Cm}_* \simeq 2.597$. At $\mathrm{Cm} > 2.597$ the solution for the eigenvalue of the first odd mode appears at $4\lambda/\mathrm{Cm}^2 > 1$. This solution with the increase of Cm in a non-monotonous way, as shown by a solid line in Fig. 2, approaches $4\lambda/\mathrm{Cm}^2 = 4$. The shapes of the odd and even modes obtained by integration of $y_{,l} = z$ and corresponding to $4\lambda/\mathrm{Cm}^2 > 1$ are shown in Figs. 3 and 4 for a large Cm value equal to 200.

In the limit $\mathrm{Cm} \to \infty$ there is an infinite series of modes with $4\lambda/\mathrm{Cm}^2 < 1$ and two modes—one even and one odd-

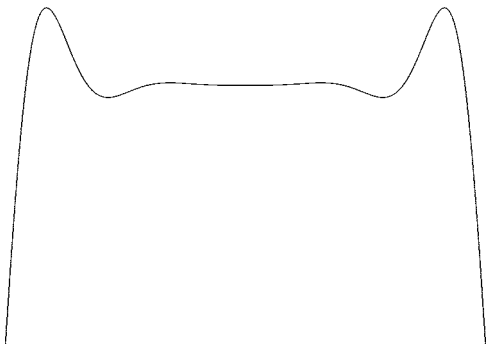

FIG. 4. First odd mode of the filament deformation. Cm=200.

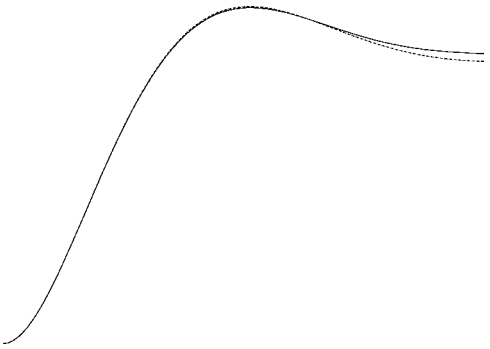

FIG. 5. Localized boundary mode (dashed line) and first odd mode of the filament deformation (solid line). Cm=50.

with $4\lambda/\mathrm{Cm}^2=4$, which cannot be obtained from the continuum limit of the infinite filament since the spectrum of the increments corresponding to the periodic modes e^{iql},

$$\lambda = -q^4 + \mathrm{Cm}\, q^2,$$

is limited from the above by $\mathrm{Cm}^2/4$. Two separate modes correspond to the modes of the deformation localized near tips of a filament. This can be illustrated considering semi-infinite filaments with $l \in (-\infty, 0)$ and boundary conditions at its right end:

$$\left.\frac{dz}{dl}\right|_{l=0} = 0, \tag{9}$$

$$\left.\left(\frac{\mathrm{d}^2 z}{\mathrm{d}l^2} + \mathrm{Cm}\, z\right)\right|_{l=0} = 0. \tag{10}$$

The decaying at the $l \to -\infty$ solution of Eq. (5) at $\vartheta = e^{\lambda t} z(l)$ reads

$$z = Ae^{\sqrt{\mathrm{Cm}}\,\alpha_1 l} + Be^{\sqrt{\mathrm{Cm}}\,\alpha_2 l}, \tag{11}$$

where

$$\alpha_1 = -i\sqrt{\frac{1+\sqrt{1-4\lambda/\mathrm{Cm}^2}}{2}}$$

and

$$\alpha_2 = i\sqrt{\frac{1-\sqrt{1-4\lambda/\mathrm{Cm}^2}}{2}},$$

and according to boundary conditions (9) and (10),

$$\alpha_1 \alpha_2 = 1. \tag{12}$$

From the dispersion relation (12) we see that the growth increment of the localized boundary deformation modes satisfies $\lambda/\mathrm{Cm}^2=1$, which corresponds to the solution of the dispersion equations (7) and (8) for the even and odd modes with the largest growth increments in the limit of large Cm.

In Fig. 5 for one-half of the filament the comparison of the localized boundary mode (11) with odd mode at Cm =50 is carried out. We see that the behavior of both is close at this value of magnetoelastic number. The even or odd modes of the deformation of the filament with finite length with $4\lambda/\mathrm{Cm}^2>1$ are close to the symmetric or antisymmetric combination of the localized boundary modes. Since they have the largest increments—namely, the localized boundary modes—they are responsible for the behavior of the filaments described below.

It is interesting to note that analysis of the growth increments for the deformation modes of spontaneously magnetized filaments in the field oriented opposite to the magnetization is close to that of superparamagnetic filaments under the action of the perpendicular field. Such an analysis based on the equations of motion of the superparamagnetic filaments [6] is carried in [16,17], where critical values of the magnetoelastic number corresponding to the neutral deformation modes [16] and their growth increments [17] are found. These results show that the stability analysis in both cases is the same if for the magnetoelastic number the substitution $\mathrm{Cm} \to 2\,\mathrm{Cm}$ is carried out.

B. Floquet analysis

According to the linear stability analysis, which shows the growth of different deformation modes of the filament, when the direction of its magnetization is opposite to the external field, we should expect the development of the deformation of the filament in an ac field, when direction of the field periodically changes between the directions along the magnetization and opposite to it. The nonmonotonous dependence of the growth increments of two localized modes on Cm shown in Fig. 2 indicates that in dependence on the Cm value and initial conditions in some range of the parameters the even mode of the filament deformation will be preferred but for some other odd mode. Since the eigenfunctions of the problem for positive and negative Cm values are different, the direct calculation of the total growth of the modes even for the steplike switching of a field from positive to negative values is not simple. Due to this, we have calculated the growth factors for the modes of the filament deformation numerically. The numerical calculation results show that in an ac magnetic field only even and odd localized modes are surviving. The slope of the dependence of the growth factors on Cm starts to increase at $\mathrm{Cm}/\sqrt{\omega} \simeq 1$. The parameter $\mathrm{Cm}/\sqrt{\omega}$ quite naturally appears at the scaling analysis of the dynamics of the filament (see Sec. III). Modes corresponding in the limit of infinite filament to the continuous spectrum are decaying for all values of Cm. The growth factors μ_F, which describe the increase of the deformation mode per period of the field according to $y_T = \mu_F y_0$, for several representative values of ω are shown in Figs. 6–8. We see that in dependence on the Cm value the most fast growing could be the even or odd localized mode. For small ω the even mode prevails for all values of the Cm number (Fig. 6). At large Cm and ω values the growth factors for both modes become practically equal (Fig. 8). In Figs. 6–8 we show the growth factors for a limited range of the magnetoelastic number due to the limited validity of the linear stability analysis.

C. Time averaging

In the case when the frequency of an ac field is enough large the behavior of the even mode in the nonlinear regime

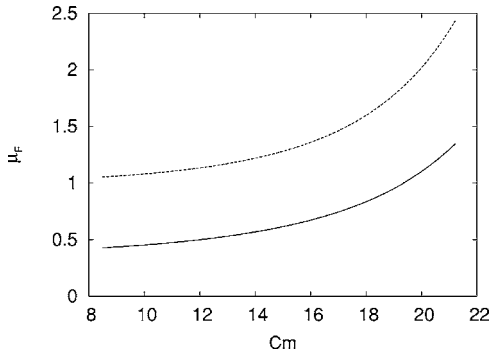

FIG. 6. Growth factor of even (dashed line) and odd (solid line) modes in an ac field in dependence on Cm. $\omega=200$.

can be considered on the basis of the time-averaging procedure. In this case we can consider the small deviations of the shape of the filament from the straight configuration characterized by its orientation angle $\beta(t)$ with the direction of an ac field (Fig. 1). Representing ϑ as $\beta+\tilde{\vartheta}$ and linearizing with the respect to $\tilde{\vartheta}$ (the tilde further is omitted) we obtain the following equation:

$$\beta_{,t}+\vartheta_{,t}=-\vartheta_{,llll}+\mathrm{Cm}\cos\omega t\cos\beta\vartheta_{,ll}$$

at boundary conditions

$$\vartheta_{,l}|_{l=-1,1}=0,$$

$$\vartheta_{,ll}|_{l=-1,1}=\mathrm{Cm}\cos\omega t\sin\beta+\mathrm{Cm}\cos\omega t\cos\beta\vartheta|_{l=-1,1}.$$

The tangent angle perturbation can be decomposed into a fast oscillating part ϑ_0 and a slowly varying part w, where ϑ_0 is a solution of the problem considered in [7]:

$$\vartheta_{0,t}=-\vartheta_{0,llll}, \tag{13}$$

$$\vartheta_{0,ll}|_{l=-1,1}=\mathrm{Cm}\cos\omega t\sin\beta, \tag{14}$$

$$\vartheta_{0,l}|_{l=-1,1}=0. \tag{15}$$

The solution of the problem (13)–(15) can be put in the form [7]

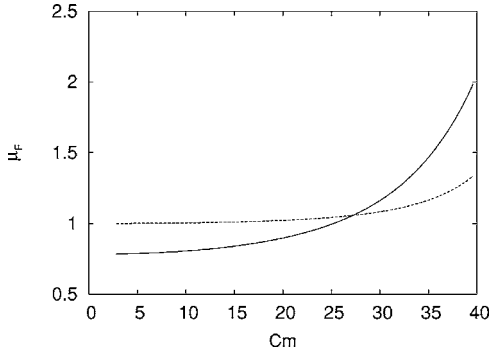

FIG. 7. Growth factor of even (dashed line) and odd (solid line) modes in an ac field in dependence on Cm. $\omega=800$.

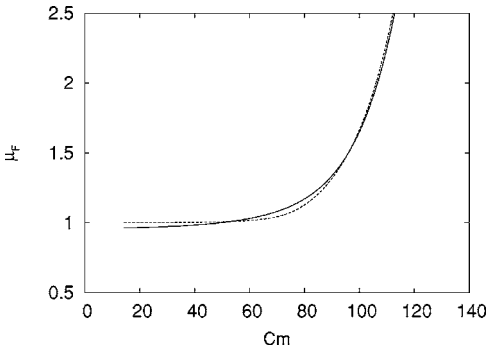

FIG. 8. Growth factor of even (dashed line) and odd (solid line) modes in an ac field in dependence on Cm. $\omega=5000$.

$$\vartheta_0=-8\ \mathrm{Cm}\sin\beta(\kappa_{1,l}(l)\cos\omega t-\kappa_{2,l}(l)\sin\omega t), \tag{16}$$

where $\kappa_{1,2}(l)$ are known functions. For the slow variable after averaging $\langle w\rangle=\int_0^{2\pi/\omega}w\,dt$ and neglecting its variation during the period of the field $2\pi/\omega$ we have the equation

$$\beta_{,t}=-\langle w\rangle_{,llll}-2\ \mathrm{Cm}^2\sin 2\beta\kappa_{1,lll}, \tag{17}$$

$$\langle w\rangle_{,l}|_{l=-1,1}=0, \tag{18}$$

$$\langle w\rangle_{,ll}|_{l=-1,1}=-2\ \mathrm{Cm}^2\sin 2\beta\kappa_{1,l}|_{l=-1,1}. \tag{19}$$

From the existence of the solution of the problem (17)–(19) we obtain the equation for the orientation angle β:

$$\frac{d\beta}{dt}=3\ \mathrm{Cm}^2\sin 2\beta\chi_1, \tag{20}$$

here, $\chi_1=\mathrm{Re}\,\chi$, where

$$\chi=2\frac{(\cosh k-1)\sin k+(1-\cos k)\sinh k}{k^3(\cosh k\cos k-1)}$$

and $k=2\omega^{1/4}e^{-i\pi/8}$.

Equation (20) has a simple physical meaning. Since the averaged per period energy of the filament can be written as

$$E=-\left\langle\frac{1}{2}\int M\cos(\beta+\vartheta)H\cos\omega t\,\mathrm{d}l\right\rangle$$

$$\sim-2\frac{C}{L}\mathrm{Cm}^2\sin^2\beta\chi_1,$$

then the equation of the motion of the filament with the rotational drag coefficient $\frac{2\zeta L^3}{3}$ reads

$$\frac{2\zeta L^3}{3}\frac{d\beta}{dt}=-\frac{\partial E}{\partial\beta}. \tag{21}$$

Equation (21) put in dimensionless form coincides with Eq. (20).

Since $\chi_1>0$ [7], then Eq. (20) shows that in an ac magnetic field of enough high frequency the angle β evolves to the value $\pi/2$. This phenomenon has the following physical explanation. For the spontaneously magnetized filament its straight configuration along the direction of an ac magnetic field during the half period when the directions of the mag-

netization of the filament and the field are opposite is energetically disadvantageous. The increase of the magnetic energy for this orientation of the field completely compensates its decrease during the second half-period, when the magnetization and field are in the same direction. Therefore it turns out from the energetical point of view advantageous to have the filament in a direction perpendicular to the field when the magnetic energy of the filament is diminishing for each half-period by the bending of the ends of the filament.

III. DYNAMICS OF FILAMENT IN AN ac MAGNETIC FIELD

A. Scaling laws

The classification of the dynamical regimes of magnetized filament in an ac magnetic field is possible by scaling arguments. In [18,19] the deformation of the semi-infinite filament under the action of the transversal force F_a applied at its end is considered. The equation for the small displacement y of the filament reads

$$y_{,t} = -y_{,llll} + \mathrm{Cm}\, y_{,ll} \tag{22}$$

at boundary conditions

$$y_{,ll}|_{l=0} = 0,$$

$$y_{,lll}|_{l=0} = \mathrm{Cm}\, y_{,ll}|_{l=0} + F_a \tag{23}$$

and initial condition $y|_{t=0}=0$. It is easy to see that the solution of the problem for $y(0,t)$ written in dimensional variables according to the scalings introduced above is

$$y(0,t) = \frac{L^3 F_a}{C\,\mathrm{Cm}^{3/2}} f\left(\frac{\mathrm{Cm}^2 tC}{\zeta L^4}\right).$$

In the limit of large t, which is equivalent to large Cm, the solution does not depend on the curvature elasticity. It means that for large x $f(x)\sim x^{1/2}$ and the following scaling law is valid [7,18,19]:

$$y(0,t) \sim \frac{F_a}{(MH)^{1/2}} \frac{t^{1/2}}{\zeta^{1/2}}.$$

In this case, since the force on the tip of the filament is due to the magnetic torque MH, the magnetic energy E_m of the deformed filament $MHy(0,t)$ scales as

$$\frac{(MH)^{3/2} t^{1/2}}{\zeta^{1/2}},$$

which according to the scales introduced above gives

$$E_m \sim \frac{C}{L}\,\mathrm{Cm}^{3/2}\left(\frac{t}{\tau}\right)^{1/2}.$$

Taking as the characteristic time scale the period of the external field we obtain

$$E_m \sim \frac{C}{L}\frac{\mathrm{Cm}^{3/2}}{(\omega\tau)^{1/2}}.$$

In the case of small Cm number or, what is equivalent, to short time intervals the deformation of the filament does not depend on the Cm number. Thus at small x, $f(x)\sim x^{3/4}$ and

$$y(0,t) \sim \frac{F_a}{C}\left(\frac{tC}{\zeta}\right)^{3/4}. \tag{24}$$

In this case for the scaling of the magnetic energy we have

$$E_m \sim \frac{C}{L}\,\mathrm{Cm}^2\left(\frac{t}{\tau}\right)^{3/4}.$$

Taking as the characteristic time scale the period of the field in this case the characteristic magnetic energy reads

$$E_m \sim \frac{C}{L}\frac{\mathrm{Cm}^2}{(\omega\tau)^{3/4}}.$$

It is the characteristic value of the energy determining the evolution of the mean orientation angle of the filament as obtained by the time averaging for the high frequencies of an ac magnetic field. We see the crossover of the dependence of the characteristic magnetic energy on the frequency with its increase from $(\omega\tau)^{-1/2}$ to $(\omega\tau)^{-3/4}$. The characteristic crossover frequency ω_* is determined by $\mathrm{Cm}/(\omega_*\tau)^{1/2}\simeq 1$. It has simple physical meaning. The scaling law $t^{3/4}$ for the displacement of the tip of filament corresponds to the balance of the external force F_a by the restoring force due to elastic deformations, which during the time t penetrates through the distance $L_e \simeq (Ct/\zeta)^{1/4}$. Force balance $Cy(0,t)/L_e^3 = F_a$ gives the relation (24). The characteristic magnetic deformation length is determined in similar way as $L_m=(MHt/\zeta)^{1/2}$. We see that in the high-frequency regime $L_e > L_m$ and the deformation is determined by the elastic deformation forces. Comparing L_e and L_m, for the characteristic crossover frequency we obtain $(\omega_*\tau)^{1/2}=\mathrm{Cm}$.

B. Numerical simulation results

Details of the dynamics of the magnetic filament in an ac magnetic field can be studied by numerical solution of Eqs. (3) and (4). The algorithm of the numerical solution is described in [6]. The boundary conditions correspond to the free and unclamped ends. As follows from the Floquet analysis in Sec. II there are two deformation modes growing under the action of an ac magnetic field. Their development is determined by the initial conditions—even or odd. In this section we illustrate the behavior of these modes in a nonlinear regime. The dynamics of the filament for the steady even oscillatory state for one period of oscillation is shown in

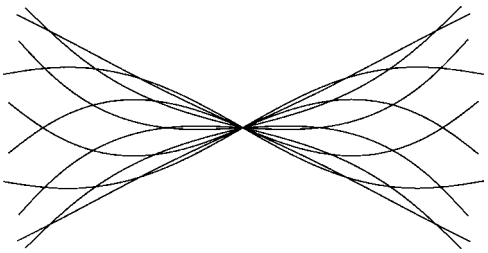

FIG. 9. Steady oscillation regime around the perpendicular direction to the field at Cm=10, ω=62.83. Configurations for one period with time step 1/100 are shown.

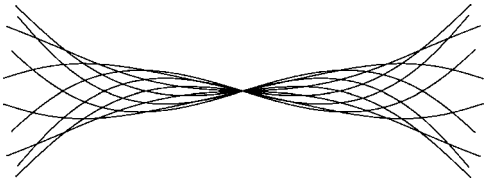

FIG. 10. Steady oscillation regime around the direction perpendicular to the field at Cm=10, ω=188.496. Configurations for one period with time step 1/300 are shown.

Figs. 9–11. We see that in a steady case the filament oscillates around its mean orientation perpendicular to the field direction. At very high frequencies of an ac magnetic field the filament is practically straight and only its tips are oscillating with the frequency of the field as is illustrated in Fig. 11. It should be remarked that if, for example, in the case shown in Fig. 11 odd initial conditions are chosen the U-like steady oscillation regime is established, which is in agreement with our analysis of the growth factors. The dynamics of the establishment of the steady state for the set of the parameters corresponding to Fig. 10 is shown in Fig. 12. To compare the dynamics of the establishment of the steady state with the predictions of Eq. (20) the tangent angle in the middle of the filament is numerically averaged per period. It is shown in dependence on dimensionless time at Cm=10 and ω=188.496 in Fig. 13. We see that the behavior of the averaged per period tangent angle in the center of the filament agrees well with the given by the solution of Eq. (20):

$$\beta = \arctan[\tan \beta_0 \exp(6\ \mathrm{Cm}^2 \chi_1) t]. \tag{25}$$

Here $6\ \mathrm{Cm}^2\chi_1$ is 1.755, obtained by the fit value of the coefficient, which corresponds reasonably well to the value 1.881 obtained according to the theoretical value of the magnetic susceptibility given in [7]. The fit for the same frequency at Cm=5 in the time interval $t \in [6;17]$ gives $6\ \mathrm{Cm}^2\chi_1$=0.493. The theoretical value obtained according to [7] in this case is 0.470. Some discrepancy of the numerical and the theoretical values for the parameter $6\ \mathrm{Cm}^2\chi_1$ may be due to the fact that values of the parameter $\mathrm{Cm}/\sqrt{\omega}$ (0.73 and 0.36), which determines the validity of the time averaging approach, are not small enough. Higher-order terms for the time-averaged equations of the relaxation dynamics of the filament will be considered in the another publication. The oscillation amplitude of the tangent angle at the filament center in dependence on the frequency for Cm=10 is shown in Fig. 14.

In the range of parameters where according to the Floquet analysis the growth of the odd deformation mode is possible at the odd initial conditions the U-like steady oscillation regime is established. This is illustrated in Fig. 15 where the

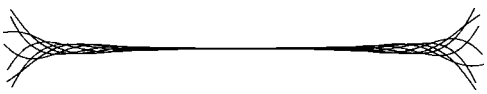

FIG. 11. Steady oscillation regime around the direction perpendicular to the field at Cm=170, ω=20195.95. Configurations for one period with time step 1/22500 are shown.

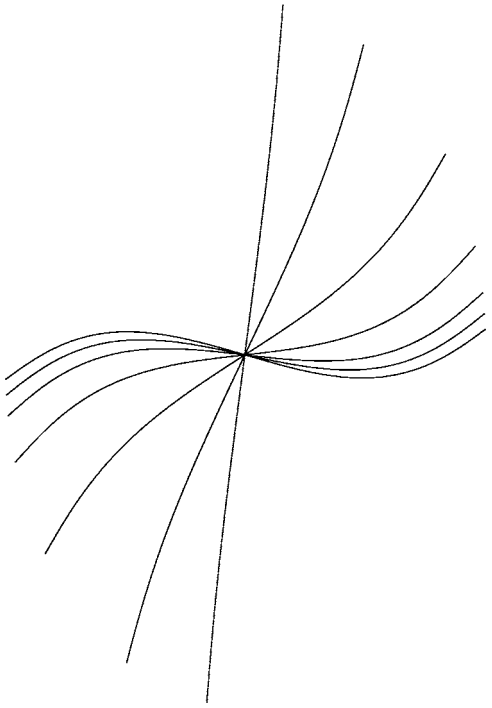

FIG. 12. Establishment of the steady oscillation regime around the direction perpendicular to the field at Cm=10, ω=188.496. Configurations are shown for $t=t_0$, t_0+15T, t_0+30T, t_0+45T, t_0+60T, t_0+75T, t_0+195T, where t_0=0.6489 and the period of the field T=1/30.

oscillation of the filament for period in U-like steady state is shown. As initial perturbation of the filament $\vartheta(l)=5\times10^{-3}f(l)$ in this case is taken, where the function $f(l)$ is defined by

$$f(l) = -2(l+1)\exp[-20(l+1)^2] - 2(l-1)\exp[-20(l-1)^2].$$

It should be remarked that if the frequency of an ac field is low enough, then at odd initial filament tangent angle perturbations a strongly bent intermediate state can form as shown in Fig. 16 for Cm=10 and ω=10. As an initial configuration in this case $\vartheta=0.1f(l)$ has been chosen. In the agreement with the Floquet analysis in the longer period of time for the

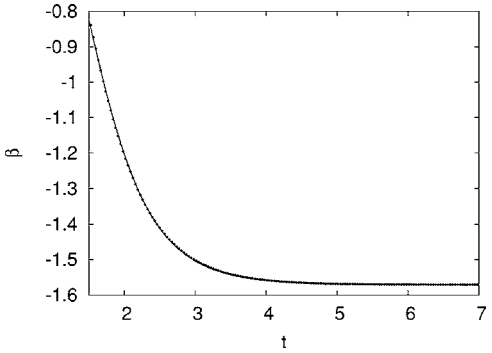

FIG. 13. Relaxation dynamics of the angle β at Cm=10, ω=188.496. Circles: numerical data. Solid line: fit by the theoretical dependence (20) at $6\mathrm{Cm}^2\chi_1$=1.755.

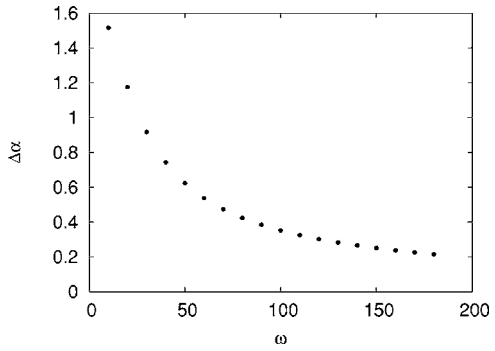

FIG. 14. Amplitude of tangent-angle steady oscillation at Cm =10.

parameters corresponding to Fig. 16 the even shape of the filament, due to the presence of the some numerical noise, develops since only it has a growth factor bigger than 1. The formation of a strongly bent intermediate state, as shown in Fig. 16, if the magnetic interaction between the tips is switched on, would presumably lead to the formation of rings of spontaneously magnetized filaments. The possibility of ring formation due to the balance of the elastic forces and the interaction between the tips of the filament is considered in [4]. Although the formation of rings is energetically possible if the filaments are long enough, nevertheless, how they overcome the energetical barrier to form the ring remains unclear yet. The results obtained here show the possibility to produce the rings by using an ac magnetic field.

Thus the numerical results show that depending on the initial conditions and the values of the parameters S-like or U-like oscillations of the filament corresponding to the localized modes of the filament deformation can be established. Direct experimental investigations of these interesting phenomena at the present moment are absent, although there are some papers [8,20] considering systems close to those considered in this work.

In [20] the Fe colloid containing long chains of ferroparticles is obtained and its magnetic susceptibility in dependence on the frequency of the ac magnetic field is explored. In [7] it was shown that experimental data obtained in [20] correspond well to the model of the semiflexible spontaneously magnetized filament. In [8] the ensemble of the Ni $90-\mu$m-size particles floating on the surface of the liquid is explored and it is observed that in an ac magnetic field the particles are chaining. This means that magnetic particle filaments are in the plane perpendicular to an ac field as predicted by our model.

Interesting is the fact that vortical surface flows are excited [8], which may be reasonably explained as arising due to oscillating tips of the filaments. The main physical difference between the model considered above and experimental realization of the chaining of the magnetic particles in the plane perpendicular to the field consists in the additional elasticity of the filaments due to the capillary forces. The modified model accounting for this additional elasticity is considered in the next sections of this work. It turns out that modified in a such way the model is sufficient to predict the length of chains formed under the action of an ac field, which depends on the frequency of the field, and to obtain a reasonable estimate for the streaming velocity of the liquid.

FIG. 15. Steady oscillation regime of the odd mode at Cm=25, ω=376.991. Configurations for one period with time step 1/600 are shown.

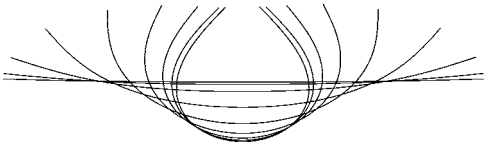

FIG. 16. Strongly bent intermediate state of the filament at Cm=10, ω=10. Configurations for times $t_0, 2t_0, 3t_0, 4t_0, 5t_0, 6t_0, 7t_0, 8t_0, 10t_0$ (t_0=1/90) are shown.

IV. MAGNETIC CHAINS ON THE SURFACE OF THE LIQUID

As a model for the chain of magnetic particles, floating on the surface of the liquid, let us take the cylindrical particle with the radius of the cross section R and a density ρ. Wetting angle of the surface is π-ϑ_S. At the capillary equilibrium the center of the particle is at the distance y_c above the surface of a liquid:

$$y_c = R\cos(\vartheta_S + \vartheta) - \sqrt{2}a\sin(\vartheta/2),$$

where ϑ is the tangent angle of the liquid surface, which it makes with the horizontal direction at the contact line, but $a=\sqrt{2\sigma/\rho_l g}$ is the capillary length of a liquid with a density ρ_l and a surface tension σ, but g is the acceleration of a free fall.

Force F per unit length acting on the particle is

$$F = 2\sigma\sin\vartheta - \rho\pi R^2 g.$$

The equilibrium position is given by the condition $F=0$. The stiffness of the interface may be then estimated as $k=-dF/dy_c|_{F=0}$ which gives

$$k = \frac{2\sqrt{2}\sigma\cos\vartheta}{\sqrt{2}R\sin(\vartheta_S+\vartheta) + a\cos(\vartheta/2)}.$$

If the particle is enough small ($R \ll a$), then $\vartheta \simeq 0$ and a simple relation for the stiffness of the filament follows: $k=2\sqrt{2}\sigma/a$. Its value in the case of water is $\simeq$566 dyn/cm^2. The equation for the small deformations of the filament floating on the surface of the liquid reads

$$\zeta y_{,t} = -Cy_{,llll} - ky. \tag{26}$$

The boundary conditions correspond to the free and unclamped ends

$$y_{,ll}|_{l=0,L} = 0,$$

$$Cy_{,lll}|_{l=0,L} = -MH\cos\omega t.$$

In the case when the term due to the restoring capillary force is absent a complex magnetic susceptibility of the filament is calculated in [7]. In the present case the complex susceptibility reads

$$\chi = -\frac{M^2L^3}{C}\frac{2}{\tilde{\gamma}^3[\cosh\tilde{\gamma}\cos\tilde{\gamma}-1]} \times[(\cos\tilde{\gamma}-1)\sinh\tilde{\gamma}-(\cosh\tilde{\gamma}-1)\sin\tilde{\gamma}],$$

where

$$\tilde{\gamma} = \left[\left(\frac{\omega\zeta L^4}{C}\right)^2 + \left(\frac{kL^4}{C}\right)^2\right]^{1/8} e^{-i(\pi/8+\alpha/4)}$$

and

$$\alpha = \arctan\left(\frac{k}{\omega\zeta}\right).$$

The mean per period magnetic energy of the filament reads

$$E = -\frac{1}{4}H^2\mathrm{Re}(\chi).$$

The expression obtained for the magnetic susceptibility has interesting features since it shows a nonmonotonous dependence of the magnetic energy on the length of the filament. Introducing the characteristic length $L_*=(C/k)^{1/4}$ and characteristic frequency $k/\zeta=\omega_*$ the dependence of the energy of the filament on its length is determined by

$$E = -\frac{1}{2}\frac{M^2H^2}{C}L_*^3\mathrm{Re}[f(\omega/\omega_*, L/L_*)],$$

where

$$f = -\frac{1}{\gamma^3\left[\cosh\left(\frac{L}{L_*}\gamma\right)\cos\left(\frac{L}{L_*}\gamma\right)-1\right]} \times\left\{\left[\cos\left(\frac{L}{L_*}\gamma\right)-1\right]\sinh\left(\frac{L}{L_*}\gamma\right) - \left[\cosh\left(\frac{L}{L_*}\gamma\right)-1\right]\sin\left(\frac{L}{L_*}\gamma\right)\right\}$$

and

$$\gamma = [(\omega/\omega_*)^2+1]^{1/8}\exp -i(\pi/8+\alpha/4).$$

The dependence of Re f on L/L_* for several values of ω/ω_* is shown in Fig. 17. We see the characteristic maxima at finite length of the filament.

These maxima presumably should determine the length of the magnetic particle chains formed on the surface of the liquid in the vertical ac magnetic field. Estimating the curvature elasticity constant of the chain as $C=\frac{m^2}{2d^2}$ [4] for the characteristic length L_* and using the estimate of the elastic constant $k=500$ dyn/cm^2 obtained above, the value of the magnetic moment of the particle, $m=2\times10^{-4}$ emu, which corresponds to a saturation magnetization of Ni particle and its diameter $d=100$ μm, we have $L_*=0.25$ mm. This according to the data in Fig. 17 corresponds at $\omega/\omega_*\simeq1$ to a chain length 2 mm. This value is reasonable from the point of view of the experiment [8].

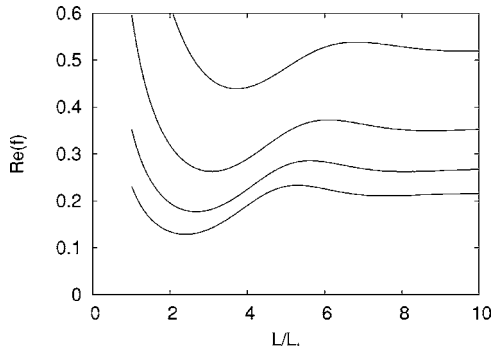

FIG. 17. Magnetic susceptibility of magnetic filament in dependence on its length for several values of the frequency of the ac field ($\omega/\omega_*=2,3,4,5$ with the frequency increasing from the upper to the lower curve).

V. STREAMING EXCITED BY OSCILLATING MAGNETIC FILAMENTS

Oscillating magnetic filaments create force on the liquid which causes its streaming. The force per unit length of the filament with the mean orientation along x axis is expressed as follows ($\vec{n}$ is the normal to the filament)

$$f_x = (Cy_{,llll} + ky)n_x.$$

Since $n_x=-y_{,l}$ then the mean per period total force acting on a liquid is

$$F_x = -\left\langle \int (Cy_{,llll} + ky)y_{,l}dl \right\rangle.$$

It can be calculated solving Eq. (26) at boundary conditions corresponding to the free and unclamped end of the semi-infinite filament $[l\in(-\infty,0)]$:

$$y_{,ll}|_{l=0} = 0,$$

$$-Cy_{,lll}|_{l=0} - MH\exp i\omega t = 0. \quad (27)$$

The solution of the problem (26) and (27) reads

$$y = v(l)e^{i\omega t}. \quad (28)$$

Here

$$v = A\exp\alpha_1 l + B\exp\alpha_2 l,$$

$$\alpha_1 = \left(\frac{k}{C}\right)^{1/4}\left[1+\left(\frac{\omega}{\omega_*}\right)^2\right]^{1/8} e^{i(\varphi+\pi)/4},$$

$$\alpha_2 = \left(\frac{k}{C}\right)^{1/4}\left[1+\left(\frac{\omega}{\omega_*}\right)^2\right]^{1/8} e^{i(\varphi-\pi)/4},$$

$$\varphi = \arctan\left(\frac{\omega}{\omega_*}\right)$$

and

$$A = -\frac{MH}{C}\frac{1}{(\alpha_1-\alpha_2)}\frac{1}{\alpha_1^2},$$

$$B = \frac{MH}{C}\frac{1}{(\alpha_1-\alpha_2)}\frac{1}{\alpha_2^2}. \tag{29}$$

For the mean per period force acting on the liquid after integration and time averaging we obtain

$$F_x = \frac{1}{2}MH\,\mathrm{Re}(v_l(0)) - \frac{k}{4}|v(0)|^2$$
$$= -\frac{(MH)^2}{2(kC)^{1/2}[1+(\omega/\omega_*)^2]^{3/4}} \times\{1-\cos(\varphi/2)[1+(\omega/\omega_*)^2]^{1/2}\}. \tag{30}$$

This force causes the streaming of the liquid along the filament in the direction of its tip. The streaming velocity can be estimated using the fundamental solution of the Stokes equation for the semispace. For the velocity of the liquid on its surface at $y=0$, due to the unit force applied at the point (0, 0, 0) in the x-axis direction, it gives

$$v_x(x,z) = \frac{1}{4\pi\eta}\left(\frac{1}{(x^2+z^2)^{1/2}} + \frac{x^2}{(x^2+z^2)^{3/2}}\right),$$

$$v_z(x,z) = \frac{1}{4\pi\eta}\frac{xz}{(x^2+z^2)^{3/2}}.$$

For the streaming velocity induced near the tip of the filament with the radius of the cross section a lying along the x-axis this gives

$$v_x(0,a) = \frac{1}{4\pi\eta}\int_{-L_{**}}^{0} f_x(x')\left(\frac{1}{(x'^2+a^2)^{1/2}} + \frac{x'^2}{(x'^2+a^2)^{3/2}}\right)dx'. \tag{31}$$

Here $L_{**}=\left(\frac{k}{C}\right)^{-1/4}\left[1+\left(\frac{\omega}{\omega_*}\right)^2\right]^{-1/8}$ is the characteristic elastic deformation penetration length given by the solution of Eq. (26).

The asymptotics of the relation (31) at $a\to 0$ gives

$$v_x(0,a) \sim \frac{f_x(0)}{2\pi\eta}\ln\frac{L_{**}}{a}.$$

Using the relation (30) and estimating $f_x(0)$ from $f_x(0)L_{**}=F_x$ we obtain the following estimate for the streaming velocity induced by the oscillating tip of the magnetized filament in an ac magnetic field:

$$v_x(0,a) = \frac{(MH)^2}{2C}L_{**}F(\omega/\omega_*)\frac{1}{2\pi\eta}\ln\frac{L_{**}}{a}. \tag{32}$$

Here

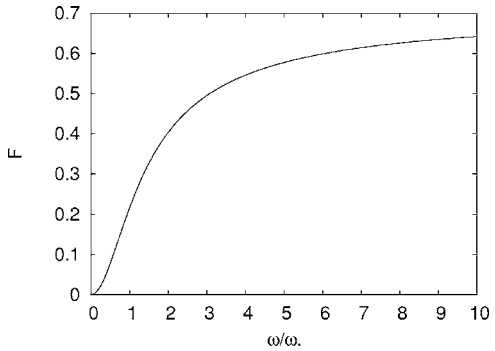

FIG. 18. Dependence of the dimensionless streaming velocity on the frequency.

$$F(\omega/\omega_*) = -\frac{1}{[1+(\omega/\omega_*)^2]^{1/2}} \times\left(1-\frac{(1+(\omega/\omega_*)^2)^{1/2}\omega/\omega_*}{\sqrt{(\omega/\omega_*)^2+[\sqrt{1+(\omega/\omega_*)^2}-1]^2}}\right). \tag{33}$$

The dependence $F(\omega/\omega_*)$ is shown in Fig. 18. We see that the force acts in the direction of the tip of the filament. Taking for the estimate of the curvature elasticity constant $C=\frac{M^2}{2}$ [4] according to the relation (32) at $H=10^2$ Oe and $\omega/\omega_*=0.1$ for the streaming velocity we have 14 cm/sec. For this estimate the value $L_*=0.25$ mm giving a reasonable optimal length of the chains is taken. The condition $\omega/\omega_*=0.1$ corresponds to the quite reasonable frequency of an ac field about 60 Hz. Although these values are close to those obtained in experiment [8], our estimate is only illustrative since at the present moment direct data on the stiffness of the filament floating on the surface of the liquid and as well the curvature elasticity of the filaments are absent. These issues create interesting problems to be explored in the future. Among them we should mention that the deformation of the surface of the liquid induced by the moving contact line at nonuniform deformation of the floating filament [21] could be important.

In spite of some mismatch of quantitative estimates with available experimental results [8] our model of the flexible magnetic filament allows us obtain some insight into the complex pattern formation phenomena of the ensemble of magnetic particles in an ac magnetic field, explain such features observed in experiment as the chain formation in the plane perpendicular to the field, the existence of the optimal length of the chains, which depends on the frequency of an ac magnetic field, the streaming of the liquid caused by the oscillating tips of magnetic filaments, and other cases.

In conclusion, we have developed a model for the nonlinear dynamics of magnetized filaments in an ac magnetic field. By a linear stability analysis we have found that the behavior of the filament in an ac magnetic field is determined by the localized boundary modes, which are separated from the deformation modes of the continuum limit. By numerical calculation of the Floquet coefficients it is shown that the localized modes are responsible for the deformation of the

filament in an ac magnetic field. Among different important phenomena, which take place in an ac magnetic field, the orientation of the filament in the direction perpendicular to the field is found by the time-averaging approach and confirmed numerically. The numerical simulation results give evidence of the possibility of ring formation by spontaneously magnetized filaments under the action of an ac magnetic field. It is illustrated that the properties of the magnetized filaments found may give the insight into the complex pattern formation phenomena of the two-dimensional ensembles of the magnetic particles observed in the experiments recently.

[1] C. Goubault, P. Jop, M. Fermigier, J. Bandry, E. Bertrand, and J. Bibette, Phys. Rev. Lett. **91**, 260802 (2003).
[2] S. L. Biswal and A. P. Gast, Phys. Rev. E **68**, 021402 (2003).
[3] R. Dreyfus *et al.*, Nature (London) **437**, 862 (2005).
[4] A. Cebers, Curr. Opin. Colloid Interface Sci. **10**, 167 (2005).
[5] S. L. Biswal and A. P. Gast, Anal. Chem. **76**, 6448 (2004).
[6] A. Cebers, J. Phys.: Condens. Matter **15**, S1335 (2003).
[7] M. Belovs and A. Cebers, Phys. Rev. E **73**, 021507 (2006).
[8] A. Snezhko, I. S. Aranson, and W.-K. Kwok, Phys. Rev. Lett. **96**, 078701 (2006).
[9] I. Drikis and A. Cebers, Magnetohydrodynamics **40**, 351 (2004).
[10] S. Childress, *Mechanics of Swimming and Flying* (Cambridge University Press, New York, 1981).
[11] S. Camalet, F. Julicher, and J. Prost, Phys. Rev. Lett. **82**, 1590 (1999).
[12] A. Cebers and I. Javaitis, Phys. Rev. E **69**, 021404 (2004).
[13] A. Cebers and I. Javaitis, Magnetohydrodynamics **40**, 345 (2004).
[14] A. Cebers, Magnetohydrodynamics **41**, 63 (2005).
[15] A. J. Levine, T. B. Liverpool, and F. C. MacKintosh, Phys. Rev. Lett. **93**, 038102 (2004).
[16] A. Cebers, J. Magn. Magn. Mater. **289**, 335 (2005).
[17] R. Dreyfus, Ph.D. thesis, l'Universite Paris VI, 2005.
[18] A. Cebers and I. Javaitis, Phys. Rev. E **70**, 021404 (2004).
[19] M. Belovs, A. Cebers, and I. Javaitis in the *15th Riga and 6th Pamir Conference on Fundamental and Applied MHD*, Riga (Jurmala, Latvia, 2005), p. 325.
[20] K. Butter *et al.*, J. Phys.: Condens. Matter **15**, S1451 (2003).
[21] P.-G. de Gennes, Fr. Brochard-Wyart, and D. Quere, *Drops, bubbles, pearls, and waves* (Belin, 2002) (in French).